X-ray diffraction and structure of water

J. Appl. Cryst. (1968). **1**, 234

X-ray Diffraction and Structure of Water

BY W. BOL

Technische Hogeschool Eindhoven, The Netherlands

(*Received* 4 *June* 1968 *and in revised form* 3 *July* 1968)

With the help of X-ray diffraction, liquid water at 25 °C has been studied. The results agree fairly well with previous work, including the work of van Panthaleon van Eck, Mendel & Boog (1957–1962). The radial distribution function obtained is in accordance with an irregular network model, resembling ice I and the high pressure modifications, ice II, ice III, ice V and ice VI. Unlike the situation in the ice structures, in water a fraction of the hydrogen bonds are broken and all hydrogen bonds have approximately the same chance of being broken. Accordingly, each molecule is not surrounded by 4 hydrogen-bonded neighbours but by a somewhat smaller number, probably 3·2 (on average); moreover, there appear to be 4·6 non-bonded neighbours at a distance of less than 4 Å from the reference molecule.

Introduction

In studies of the water structure during the last decade, marked results have been achieved. Yet several important problems remain, whose solution is urgent for several reasons, the most important of which is that our colleagues in protein research have made tremendous progress during the same period of years. Since it may be said that life takes place at the interface of proteins and water, we must admit that our half of the work has lagged behind. Therefore, it is of some importance that great efforts be made towards an adequate description of the water structure.

In this article we will sort out one problem that exists in this field, namely the discrepancy between the X-ray work of some Dutch workers on the one hand, *viz.* van Panthaleon van Eck, Mendel & Boog (1957), Heemskerk (1962), and the work of Morgan & Warren (1938), Narten, Danford & Levy (1967) on the other. Furthermore, we hope to start a final discussion on the discrepancy which exists between the cluster model and the irregular network model both of which are used for the water structure.

In this article we will adopt the irregular network model because it is the simpler of the two and because recently the criticisms of Perram & Levine (1967) and of Luck (1967*a*) have weakened the basis of the cluster model. It is true, however, that Luck himself (1967*b*) gives a drawing of a cluster model with a fraction of disrupted hydrogen bonds, which is much smaller than in the model of Némethy & Scheraga (1962). In this case it is difficult to believe that the thin film with disrupted hydrogen bonds, present around each cluster (as suggested by Luck), will not be bridged over occasionally by the formation of hydrogen bonds between water molecules of different clusters, so giving rise to a more or less irregular network throughout the liquid.

An irregular network model must account for the fluidity of water even at low temperatures; *e.g.* at −10 °C the viscosity of water is as low as 0·027 poise. We think the fluidity is caused by the inversion of triply bonded water molecules *via* the sp^2 hybrid (see Fig. 1). Triply bonded water molecules occur abundantly in liquid water. As we will see later, at 25 °C, 41%, and at −10 °C still more than 20%, of the water molecules are triply bonded. Half the number of these have a pair of free electrons, which allows reorientation as illustrated in Fig. 1. Such reorientation requires only a slight movement (0·5–1·0 Å) of one molecule and it will therefore be a very fast process, so that after some time hardly any of the original hydrogen bonds remain. In this way we have described a network with a high degree of mobility without many hydrogen bonds being disrupted at a time. It is very likely that a water molecule can assume the sp^2 hybrid form, since in $(NH_3)_2.H_2O$ each water molecule is surrounded by five ammonia molecules. Three of these lie in the same plane as the water molecule, and the other two on either side (Siemons & Templeton, 1954). In fact, there are also water molecules linked to their neigh-

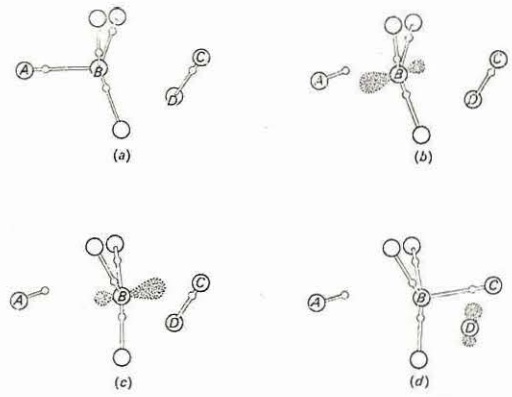

Fig. 1. Inversion of triply bonded water molecules. (*a*) Detail of network of water molecules. Hydrogen bonds with other molecules are omitted. (*b*) Hydrogen bond between *A* and *B* is disrupted. (*c*) Molecule *B* is inverted. (*d*) Hydrogen bond is established between *B* and *C*, leaving molecule *D* with a lone pair of electrons and *A* with a free OH group.

bours by two, one or no hydrogen bonds. These are even more mobile than triply bonded molecules, and contribute to the fluidity especially at higher temperatures.

Experimental

In our experiments we worked with an X-ray camera for liquids, diagrammatically represented in Fig. 2. The specimen is a vertical jet of water, about 0·5 mm in diameter. The X-rays used are of the Mo $K\alpha$ type with balanced filter monochromation in the secondary beam as discussed by Bol (1967). The specimen is in a hydrogen atmosphere. The intensity of the diffracted radiation is measured at preset diffracting angles in the horizontal plane. The measurements are carried out at angles with a fixed interval of $s=(4\pi \sin\theta)/\lambda$, λ being the wavelength of the X-rays in Å and 2θ the diffracting angle. After correction for absorption and polarization the intensity is multiplied by the appropriate scale factor calculated by the method of Krogh-Moe (1956).

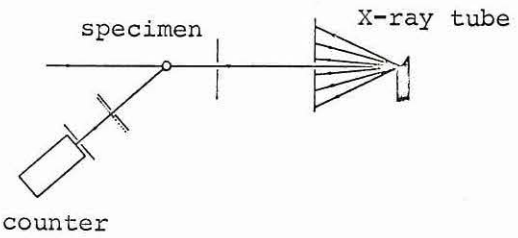

Fig. 2. Diagrammatic representation of the diffraction apparatus.

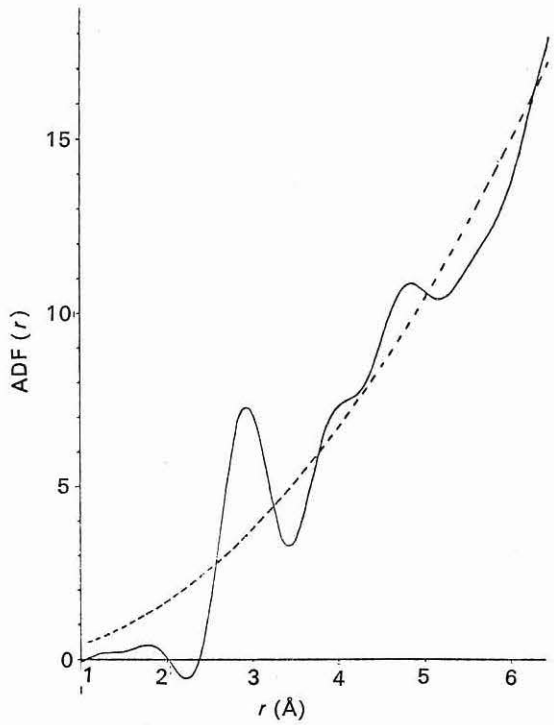

Fig. 3. Experimental atomic distribution function (ADF) of water at 25 °C.

The intensity obtained is used to calculate the radial distribution function or atomic distribution function (ADF)*. The ADF is a function of the radius r and ADF(r)dr equals the number of atoms whose internuclear distances, from some reference atom, lie between r and $r+dr$.

The 'local density' $\varrho(r)$ is related to the ADF as follows: $\mathrm{ADF}(r)=4\pi r^2\varrho(r)$. The X-ray intensity, measured and calculated as above, is related to the distribution function by the expression (James, 1962):

$$s\frac{I(s)-f^2}{f^2}=\int_0^\infty 4\pi r(\varrho(r)-\varrho_0)\sin sr\,dr \qquad (1)$$

where ϱ_0 is the mean density in atoms per Å^3 and f is the atomic scattering factor, in our case calculated from the electron density function of water as given by Bishop, Hoyland & Parr (1963). The method of calculation was taken from James (1962), p. 125.

The ADF is implicitly given by (1). It can be made explicit by Fourier transformation of (1):

$$4\pi r(\varrho(r)-\varrho_0)=\frac{2}{\pi}\int_0^\infty s\frac{I(s)-f^2}{f^2}\sin sr\,ds\,. \qquad (2)$$

Unfortunately, $I(s)$ is not known in the whole interval from $s=0$ up to $s=\infty$, but only up to a certain $s_{\max}$. Therefore it is better not to use (2) but to start from (1), multiply both sides by $\sin sr'\,ds$, r' being a new parameter with the dimension of a radius. Both sides of (1) are then integrated from $s=0$ up to $s=s_{\max}$ and the sequence of the two integrations on the right hand side is inverted. In this way we obtain

$$\int_0^{s_{\max}} s\frac{I(s)-f^2}{f^2}\sin sr'\,ds=\int_0^\infty 4\pi r(\varrho(r)-\varrho_0)\times\int_0^{s_{\max}}\sin sr\sin sr'\,ds dr\,. \qquad (3)$$

We can say that (3) gives a relationship between the experimental ADF

$$r\cdot\frac{2}{\pi}\int_0^{s_{\max}} s\frac{I(s)-f^2}{f^2}\sin sr\,ds+4\pi r^2\varrho_0$$

and the real $\mathrm{ADF}=4\pi r^2\varrho(r)$.

Equation (3) makes it possible to check whether a supposed model of the liquid is endorsed by experiment or not. Of course it is not possible to calculate the real ADF with the help of (3). The experimental ADF, which was obtained from our measurements of water at 25 °C, is given in Fig. 3. The maximum value of s, at which we have measured the intensity is $s=7{\cdot}6$. This curve is consistent with previously published curves, *e.g.* Narten, Danford & Levy (1967).

---

* Actually this only holds for monatomic liquids. We will consider water as a quasi monatomic liquid and the water molecule as a quasi atom.

It is worth noting that the results of some Dutch workers *viz.* van Panthaleon van Eck *et al.* (1957) and of Heemskerk (1962) have a quite different aspect. They have, however, published curves of a different nature. They calculated what they called an electron distribution function (EDF) which is a one-dimensional Patterson function with the formula

$$W(r)=\frac{2}{\pi}\int_0^{\infty} s(I(s)-f^2)\sin sr\,ds\,. \qquad (4)$$

An integral equation analogous to (3) can be produced:

$$\int_0^{s_{max}} s(I(s)-f^2)\sin sr'\,ds=\int_0^{\infty} 4\pi r(\varrho(r)-\varrho_0) \times\int_0^{s_{max}} f^2\sin sr\sin sr'\,dsdr\,, \qquad (5)$$

enabling one to check a proposed model as with (3).

From a mathematical point of view both methods are equivalent. The EDF method, however, has the disadvantage that the interpretation is more difficult. In Fig. 4 we have given the $W(r)$, calculated from the same intensity measurements as were used for the ADF of Fig. 3. This curve is in excellent agreement with the curves of van Panthaleon van Eck and Heemskerk.

In the following sections we will work with the commonly adopted ADF method.

In the irregular network theory water is composed of molecules connected to each other by hydrogen bonds, thus forming a network of molecules extending throughout the whole liquid as described by Pople (1951) and Bernal (1965).

This network is irregular, which means that the local configuration is different in every place, so every configuration that is possible with water molecules is found at some place at some time. It is interesting to note that a number of possible configurations occur in the many modifications of ice. Kamb & Datta (1960), Kamb, Kamb & Davis (1964), Kamb (1965) have determined the structure of ice II, III, V, VI and VII. Together with the two low pressure modifications of ice which were already known, we now have at our disposal the data of seven ice modifications. In six of them each water molecule has four nearest neighbours at a minimum distance of 2·725 Å and a maximum distance of 2·891 Å. These are the four hydrogen-bonded neighbours available to a water molecule. In Fig. 5 we have constructed histograms of the number of molecules as a function of the distance from a reference molecule.

Between two adjacent hydrogen bonds in ice there appear to be a wide variety of angles, as can be seen in Table 1. Therefore, we suppose that in water, too, there are a wide variety of angles between the hydrogen bonds. The mean angle is about 109°.

It can also be seen from Fig. 5 that in ice I the second nearest neighbours are at 4·5 Å, but in other modifications smaller distances are found. This is due to the above-mentioned fact, that the bond angles vary strongly without any great variation of bond length, *e.g.* the smallest angle, 76°, corresponds to the distance of 3·5 Å. Many of the molecules which are about

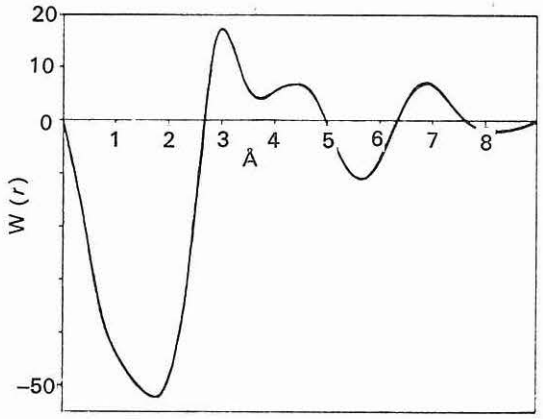

Fig. 4. Electronic distribution function $W(r)$ of liquid water at 25°C. Calculated from the same experimental data as the ADF of Fig. 3.

Table 1. *The angles between adjacent hydrogen bonds in ice*

There are six angles for each water molecule. The water molecules with different crystallographic positions are mentioned individually.

Modification of ice	Angles (°)					
I (hex)	109·4	109·4	109·4	109·5	109·5	109·5
I (cub)	109·5	109·5	109·5	109·5	109·5	109·5
II	85·3	88·3	115·1	115·5	125·6	129·4
	80·3	98·7	107·4	119·2	124·5	127·2
III	86·9	99·4	107·7	107·7	129·4	129·4
	91·6	94·6	97·3	102·9	112·9	141·7
V	86·0	86·0	97·8	127·6	130·6	130·6
	86·6	88·2	112·6	114·3	116·5	127·6
	85·3	89·3	101·8	102·2	131·6	134·9
	86·9	87·9	92·0	123·9	125·8	128·5
VI	76·1	76·1	128·3	128·3	128·3	128·3
	76·2	90·2	90·2	128·1	128·2	128·2

3·5 Å apart, however, are not second nearest neighbours in the sense that both are linked by a hydrogen bond to the same molecule. This group of extra neighbours, which does not exist in ice I, plays an important role in the water structure, as mentioned already by Morgan & Warren (1938). Apparently these are van der Waals type neighbours, which means that the van der Waals attraction is in equilibrium with the Born repulsion. In a complicated structure it is not possible to indicate which molecule is a van der Waals neighbour and which is not. We will limit the van der Waals neighbours to the group of non hydrogen-bonded molecules, which are less than 4 Å from the reference molecule. This value of 4 Å is completely arbitrary. We have chosen it because the repulsive force of the reference molecule is likely to become negligible above 4 Å.

In Table 2 we have given the number of van der Waals neighbours defined in this way and the number of 'second neighbours' which are included.

When the configuration of the van der Waals neighbours around a molecule in any of the ice structures is closely examined, there appears to be no such simple arrangement as that suggested by van Panthaleon van Eck, Mendel & Fahrenfort (1958), Narten *et al.* (1967) and Pauling (1960). There is, however, a marked tendency for the van der Waals neighbours to be found in strings of molecules, which lie in or near the perpendicular plane which bisects the line between two hydrogen-bonded water molecules. A detail of the ice V model is shown in Fig. 7, in which such a string assumes the form of an eight-membered ring.

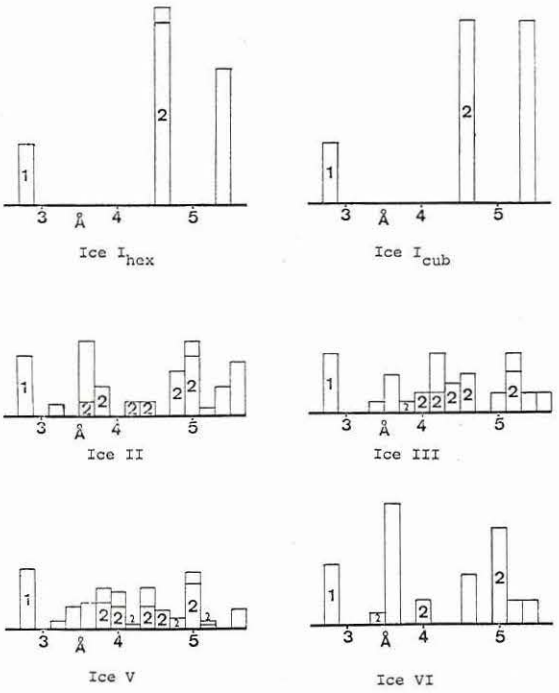

Fig. 5. Statistics of the distribution of intermolecular distances in six ice modifications. First neighbours are indicated by 1; second nearest neighbours by 2.

Table 2. *Number of van der Waals neighbours in ice*

	Number of neighbours between 3·2 and 4·0 Å	Number of 'second neighbours' included in the figures (column 1)
Ice I	0	0
Ice II	8	3
	8	3
Ice III	4	0
	5	1
Ice V	8	2
	9	3
	9	3
	10	3
Ice VI	10	2
	12	4

In this section we have omitted ice VII, the densest form of ice (density = 1·66 g.cm^{-3}). In ice VII each molecule has eight neighbours at 2·86 Å. We suppose this configuration to be so unfavourable at low pressures that it is unlikely to occur in liquid water.

Interpretation of experimental ADF and water structure

Nearest neighbours

In Fig. 3 a marked peak near 2·9 Å indicates the nearest neighbour position in liquid water. For these neighbours we adopt a distribution function which may be given by

$$4\pi r^2\varrho(r) = N \cdot \frac{r}{r_0} \cdot \frac{a}{\sqrt{\pi}} \exp\left(-(r-r_0)^2a^2\right). \qquad (6)$$

N is the number of nearest neighbours at a mean distance r_0, a is related to the mean square deviation of the distance between two neighbouring atoms $\overline{t^2}$, by $2\overline{t^2} = 1/a^2$. As the temperature factor B equals $4\pi^2\overline{t^2}$ it follows that $a^2 = 2\pi^2/B^*$. After inserting the $\varrho(r)$ obtained from (6) into (3) (with $\varrho_0 = 0$ and $s_{max} = 7{\cdot}6$) we get a transformed function for the nearest neighbours that can be compared directly with the experimental ADF. In this way we have collected the values of B and N, each set giving an optimum fit for some value of r_0. This collection is given in Table 3.

In Fig. 8 a comparison of the experimental ADF with the calculated function is shown for the case $r_0 = 2{\cdot}86$. It can be seen that several details of the ADF are due to spurious maxima in the function of nearest neighbours. The rest of the ADF, which describes all non-hydrogen-bonded molecules, is a very smooth function with only one detail at about 4·7 Å.

* In crystal analysis the formula $B = 8\pi^2\overline{u^2}$ is used. See *International Tables* (1962) and James (1962) p. 23. Here $\overline{u^2}$ is the mean square displacement of a single atom, so that $2\overline{u^2} = \overline{t^2}$.

Table 3. *Values of B and N which yield the curve best fitting the experimental curve for a number of values of* r_0

r_0	N	B
2·83	2·69	0·75
2·84	2·88	0·87
2·85	3·08	1·00
2·86	3·30	1·12
2·87	3·52	1·22
2·88	3·76	1·33
2·89	3·98	1·46
2·90	4·15	1·56
2·91	4·28	1·70

Which of the alternatives in Table 2 should be chosen cannot be concluded from the X-ray data. The best fit is obtained for $r_0=2{\cdot}86$ and the fit deteriorates on either side of this value, as can be seen in Fig. 9. It is probable that r_0 is between 2·85 Å and 2·89 Å with N between 3·1 and 3·98, which gives a fraction of unbroken hydrogen bonds between 0·77 and 1·0, at 25 °C.

In order to get a more precise picture it is necessary to make use of data from other fields of physical chemistry such as the Raman spectroscopical results of Walrafen (1966) and the ultraviolet measurements of Stevenson (1965).

In addition, an assumption is made that all bonds in the network have the same probability of being broken. This gives: a fraction of f^4 molecules with four hydrogen bonds (f is the fraction of unbroken bonds); $4f^3(1-f)$ molecules with three bonds; $6f^2(1-f)^2$ molecules with two bonds; $4f(1-f)^3$ molecules with only one hydrogen bond; and $(1-f)^4$ of monomer molecules. From Raman spectra Walrafen (1966) has calculated the fraction of quadruply bonded molecules as a function of temperature. From these data f can be calculated and hence the fraction of each of the five species in water, as a function of temperature (Fig. 10).

Stevenson (1965) has calculated the concentration of monomer from ultraviolet measurements. His data for a temperature of 23·5 °C are in agreement with those of Walrafen, but at higher temperatures the concentration of monomer is smaller than calculated from Walrafen as above. This is an indication that the above assumption is not really valid, but it can be used as a reasonably good approximation, especially at lower temperatures.

From Fig. 10 we see that $f=0{\cdot}80$ at 25 °C, and from Table 3 that $r_0=2{\cdot}85^5$ Å and $B=1{\cdot}06$ Å^2. The value quoted for B of a hydrogen-bonded molecule in crystalline materials is usually substantially higher than

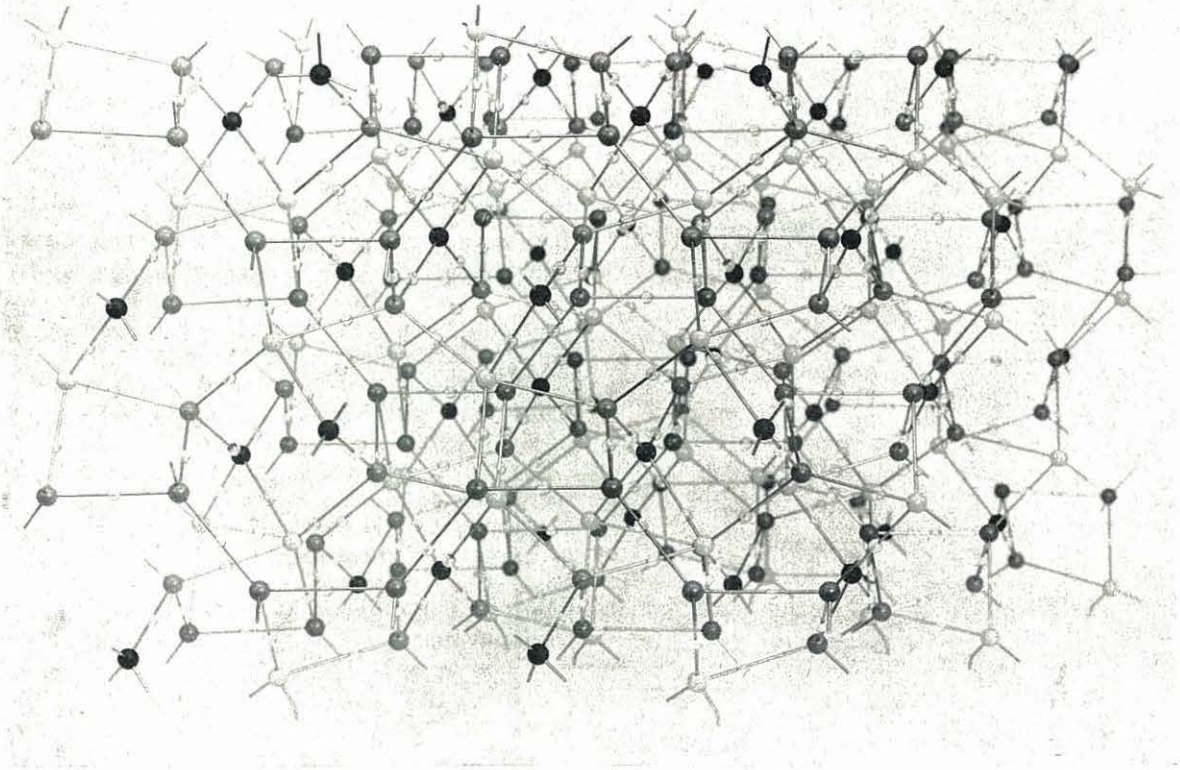

Fig. 6. Crystal model of ice V.

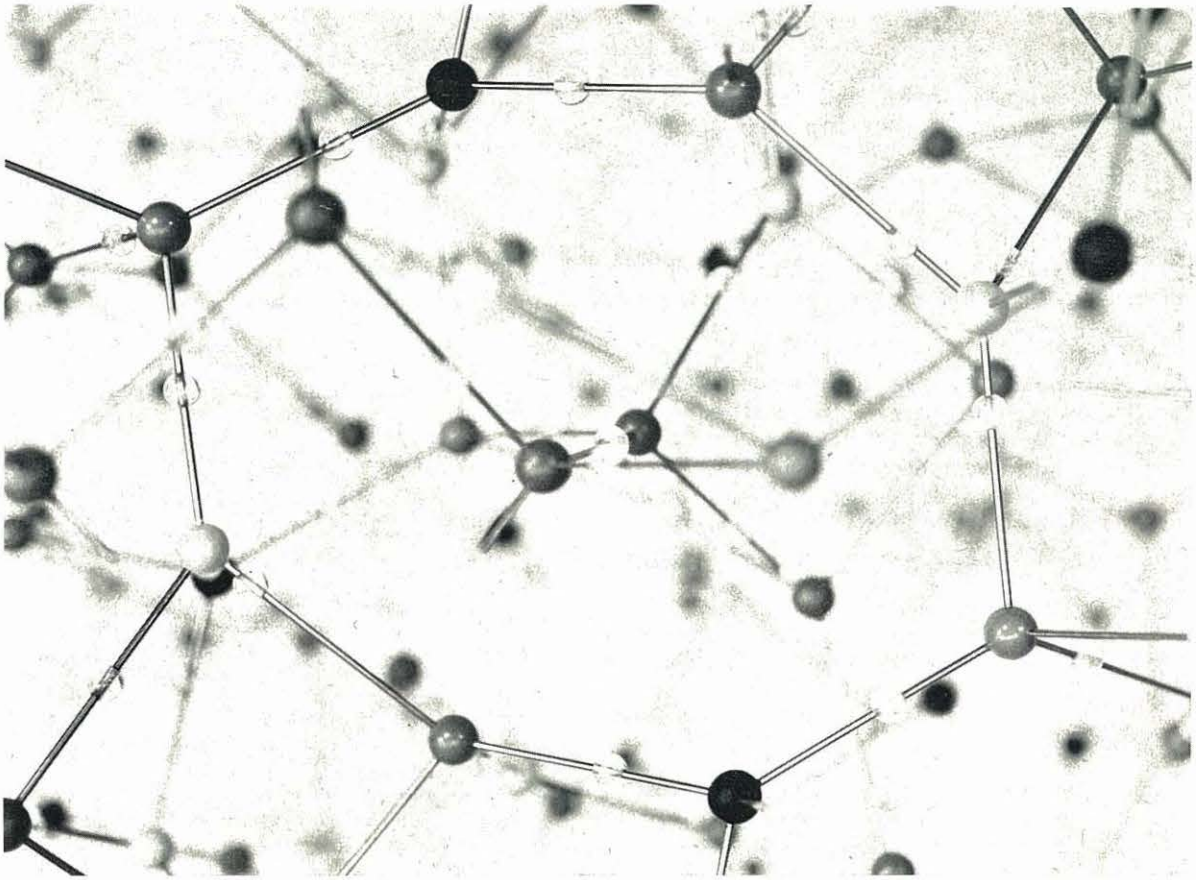

Fig. 7. Detail of the ice V model of Fig. 6. Eight membered ring encircling a hydrogen bond between two molecules in the centre.

this. This is possibly due to the fact that bending vibrations do not contribute to the nearest neighbours peak in the ADF curve. Therefore the value of B which we have found can be related only to the amplitude of the O–O stretching vibration.

Second nearest neighbours

In ice I where $f=1$, each molecule has 12 second nearest neighbours. In water, with $f=0{\cdot}80$, the number of second nearest neighbours is $12f^2=7{\cdot}68$.

The mean distance between second nearest neighbours is determined by the mean angle between two bonds (109°) and is calculated to be 4·66 Å. The ADF (Fig. 8) shows a marked peak near 4·66 Å. The shape of this peak suggests that the bond angles occurring in water deviate less from the mean value than do the bond angles in the high pressure forms of ice, where angles of about 109° are rather scarce (see Table 1). It is, however, not possible to obtain exact data on this point from the ADF.

It must be expected that half the total number of second nearest neighbours, *i.e.* 3·8, are closer than 4·66 Å to the reference molecule. Together with the 3·2 nearest neighbours this amounts to 7 molecules between $r=0$ and $r=4{\cdot}66$ Å. From integration of the experimental ADF the total appears to be 13·4. So there are 6·4 extra neighbouring molecules present within a distance of 4·66 Å.

Van der Waals neighbours

The high number of extra neighbouring molecules mentioned above suggests that there are a considerable number of van der Waals neighbours. The number of these can be obtained by integrating the ADF over the correct interval, in which case close species of 'second neighbours' are included. This is because close species of second nearest neighbours are likewise subjected to van der Waals and Born forces and therefore we must include them in order to get an adequate picture.

Integration of the experimental ADF from zero up to $r=4{\cdot}0$ Å yields a number of 7·8 molecules. This number includes 3·2 nearest neighbours, leaving 4·6 van der Waals neighbours. This number lies between that for high pressure ice and low pressure ice, just as was the case with the statistical fluctuations in the bond angles.

It must be emphasized that the number of van der Waals neighbours around the quadruply bonded molecules will be less than 4·6 and that around the molecules with fewer hydrogen-bonded neighbours it will be above 4·6.

Conclusion

In this paper we have come to the conclusion that water at 25 °C can be described as a network of molecules linked to each other by hydrogen bonds of length 2·85 [5]Å. A fraction of 20% of the bonds have been broken, thus leaving a mean number of 3·2 nearest neighbours for each molecule. In addition, each molecule has a mean number of 4·6 van der Waals neighbours. The local situation in water is intermediate between the situation in low pressure ice and in its high pressure modifications.

The author records thanks to Professor C.L. van Panthaleon van Eck for many fruitful discussions, to Mr G.J.A. Gerrits for his contribution to the experimental work and the computer programming and to Mr H.W. Maathuis for the making the crystal structure models.

References

BERNAL, J. D. (1965). *Liquids: Structure, Properties, Solid Interactions*. Ed. T. HUGHEL, p. 45. Amsterdam: Elsevier.
BISHOP, D. M., HOYLAND, J. R. & PARR, R. G. (1963). *J. Mol. Phys.* **6**, 467.
BOL, W. (1967). *J. Sci. Instrum.* **44**, 736.
HEEMSKERK, J. (1962). *Rec. Trav. chim. Pays-Bas*, **81**, 904.
International Tables for X-ray Crystallography (1962). Vol. II, p. 241. Birmingham: Kynoch Press.

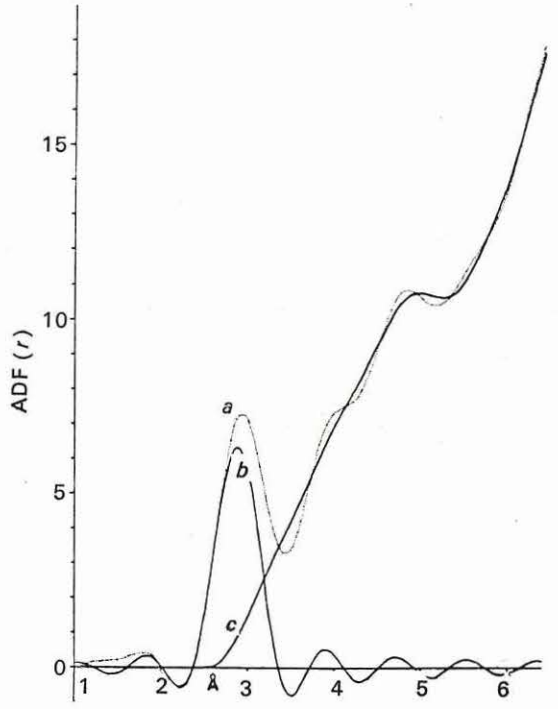

Fig. 8. Analysis of the experimental ADF. Curve (*a*) experimental ADF as in Fig. 3, curve (*b*) contribution to the ADF of 3·3 neighbours at 2·86 Å, curve (*c*) contribution of all other molecules.

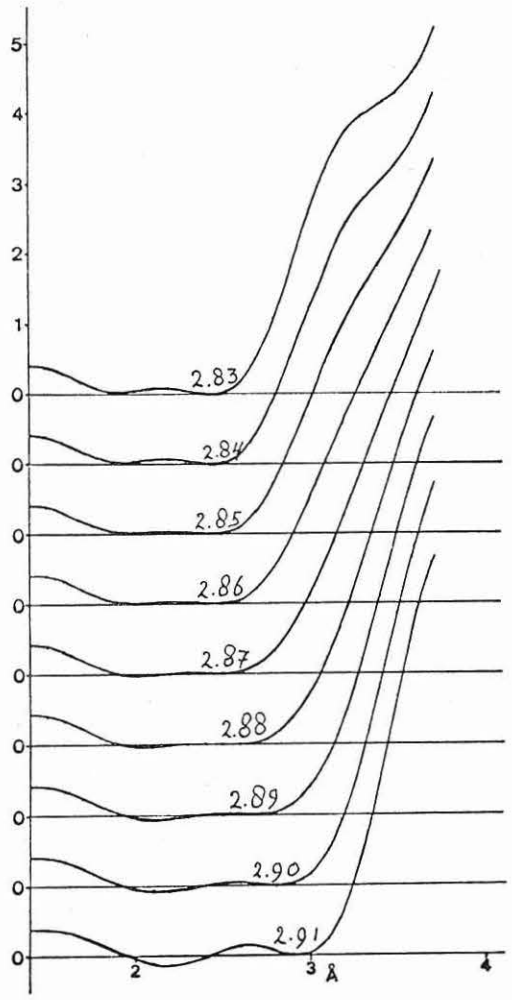

Fig. 9. The experimental ADF minus the calculated function of nearest neighbours. The nine curves correspond to the nine possibilities mentioned in Table 3. The fit of the experimental and calculated curves is good when the difference is zero over a wide range of distances.

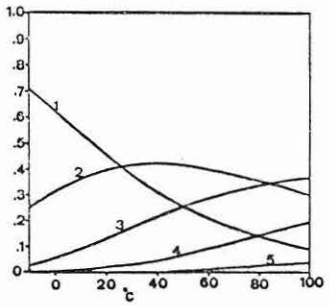

Fig. 10. Fraction of various species present in water as a function of temperature. Curve 1: quadruply bonded water molecules, curves 2, 3, 4 and 5: triply, doubly, singly and non-bonded water molecules respectively. Calculated from the data of Walrafen (1966).

JAMES, R. W. (1962). *The Optical Principles of Diffraction of X-rays*, p. 477. London: Bell.
KAMB, W. B. (1964). *Acta Cryst.* **17**, 1437.
KAMB, W. B. (1965). *Science*, **150**, 205.
KAMB, W. B. & DATTA, S. K. (1960). *Nature, Lond.* **187**, 140.
KAMB, W. B. & DAVIS, B. L. (1964). *Proc. Nat. Acad. Sci. Wash.* **52**, 1433.
KAMB, W. B., PRAKASH, A. & KNOBLER, C. (1967). *Acta Cryst.* **22**, 706.
KROGH-MOE, J. (1956). *Acta Cryst.* **9**, 951.
LUCK, W. A. P. (1967*a*). *J. Phys. Chem.* **71**, 459.
LUCK, W. A. P. (1967*b*). *Disc. Faraday Soc.* **43**, 115.
MORGAN, J. & WARREN, B. E. (1938). *J. Chem. Phys.* **6**, 666.
NARTEN, A. H., DANFORD, M. D. & LEVY, H. A. (1967). *Disc. Faraday Soc.* **43**, 97.
NÉMETHY, G. & SCHERAGA, H. A. (1962). *J. Chem. Phys.* **36**, 3382.
PANTHALEON VAN ECK, C. L. VAN, MENDEL, H. & BOOG, W. (1957). *Disc. Faraday Soc.* **24**, 200.
PANTHALEON VAN ECK, C. L. VAN, MENDEL, H. & FAHRENFORT, J. (1958). *Proc. Roy. Soc.* A**247**, 472.
PAULING, L. (1960). *The Nature of the Chemical Bond*, p. 473. Ithaca, New York: Cornell Univ. Press.
PERRAM, J. W. & LEVINE, S. (1967). *Disc. Faraday Soc.* **43**, 131.
POPLE, J. A. (1951). *Proc. Roy. Soc.* A**205**, 163.
SIEMONS, W. J. & TEMPLETON, D. H. (1954). *Acta Cryst.* **7**, 194.
STEVENSON, D. P. (1965). *J. Phys. Chem.* **69**, 2145.
WALRAFEN, G. E. (1966). *J. Chem. Phys.* **44**, 1546.

J. Appl. Cryst. (1968). **1**, 241

Characterization of Phases in the 50-60 at. % Te Region of the Bi-Te System by X-ray Powder Diffraction Patterns

BY R. F. BREBRICK

Lincoln Laboratory, Massachusetts Institute of Technology, Lexington, Massachusetts* 02173, *U.S.A.*

(*Received* 22 *July* 1968 *and in revised form* 9 *September* 1968)

Samples in the Bi–Te system containing 59·0, 58·0, 57·0, 55·0, 51·0, and 50·0 at.% Te, in addition to 5 samples within the Bi_2Te_3 homogeneity range, have been equilibrated near 525 or 450 °C and room temperature powder diffraction patterns taken. There are now 4 known phases in the 50–60 at.% Te region. The 59·0 and 58·0 at.% samples are two phase at 525 °C. The 57·0 and 55·0 at.% samples are new phases with hexagonal parameters, $a = 4{\cdot}4106 \pm 0{\cdot}0002$ Å, $c = 54{\cdot}330 \pm 0{\cdot}003$ Å and $a = 4{\cdot}4214 \pm 0{\cdot}0004$ Å, $c = 78{\cdot}195 \pm 0{\cdot}012$ Å, respectively. The 51·0 and 50·0 at.% samples are two-phase at 525 °C. At 450 °C the 51·0 at.% sample is single phase while the 50·0 at.% sample probably is not. The common indexing scheme for the 50·0 and 51·0 at.% samples is different from those for the 55·0 and 57·0 at.% samples. For the 51·0 at.% sample $a = 4{\cdot}4296 \pm 0{\cdot}0002$ Å and $c = 24{\cdot}017 \pm 0{\cdot}001$ Å. The 00*l* lines for all these phases vary strongly with composition and those near $d = 9$ and 5 Å are isolated enough to provide a convenient way of distinguishing among the various phases. The results are discussed in terms of other phase-diagram information. They are inconsistent with Stasova's correlation between composition and powder-pattern indices for the Bi–Te, Bi–Se, and Sb–Te systems.

Introduction

In conjunction with a recent determination of Te_2-partial pressures in the Bi–Te system (Brebrick, 1968), we have taken X-ray powder diffraction patterns for a number of compositions between 50 and 60 at.% Te. For powders equilibrated at 525 °C we find two new phases for 55·0 and 57·0 at.% Te samples and are able to index the patterns in the hexagonal system. The results are consistent with, and extend, the phase-diagram information obtained from the partial pressure measurements. They are inconsistent with Stasova's model (Stasova, 1964, 1967; Stasova & Karpinskii, 1967) of structures in the Bi–Se, Bi–Te, and Sb–Te systems. Moreover, we find that certain prominent lines shift strongly with composition, thereby providing a convenient means for differentiating among a set of phases with powder patterns that are generally very similar.

* Operated with support from the U.S. Air Force.

Experimental

Each sample consisted of about 15 g of the 99·99% pure elements weighed to the nearest 0·1 mg, melted by heating to 700 °C in a sealed, evacuated silica tube, quenched, ground to a 1 mm maximum powder size, and annealed for 160 hr at 525 °C. A more detailed description is given elsewhere (Brebrick, 1968). Some of the samples were subdivided for use in the partial pressure measurements. About 3 g of each sample were then ground to 44 μ and reannealed for 160 hr at 525 °C in a sealed, evacuated silica tube. In this manner samples containing 55·0, 57·0, 58·0, and 59·0 at.% Te were prepared. For 5 samples with compositions within the homogeneity range of the Bi_2Te_3 phase the final anneal was shortened to 3 hr. For a 51·0 at.% sample the final anneal was at 450 rather than 525 °C. Second 55·0 and 57·0 at.% samples with 0·177 mm particle size were annealed for 160 and 348 hr, respectively, at 525 °C before grinding to 44 μ and reannealing for